US-APWR

Core Inlet Blockage Test for Test Conditions with Design Changes in Recirculation Water Flow Path to Refueling Water Storage Pit

Non-Proprietary Version

June 2013

Revision History

Revision	Page	Description
0	All	Original issued
1	General	Abbreviation is corrected in “List of Tables”, “List of Figures” and “List of Acronyms”.
	General	Corrected other editorial errors. Note that revision bar related to these editorial corrections is removed.
	17	Editorial correction. Added “TM (Trade Mark)” to “NUKON”.
	21	Added weight of particulate debris to each test case
	23	Corrected to the appropriate sentences
	27	Added explanation for weight of fibrous debris.
	30	Corrected to the appropriate sentences
	31	Added explanation for weight of fibrous debris.
	35	Added explanation for weight of fibrous debris.
	41	Added explanation for weight of fibrous debris.
	45	Added explanation for weight of fibrous debris.
	49	Added explanation for weight of fibrous debris.
	54	Added explanation for weight of fibrous debris.
	58	Corrected to the appropriate sentences
	59	The revision number of Reference 1.0-2, 1.0-3 and 6.4-1 were updated.
	60	Added “TM (Trade Mark)” to “NUKON”.

Mitsubishi Heavy Industries, Ltd.
16-5, Konan 2-chome, Minato-ku
Tokyo 108-8215 Japan

Abstract

The US-APWR plant is designed to facilitate core cooling during a postulated loss-of-coolant-accident (LOCA). The chemical precipitate, fibrous and particulate debris assumed to be generated in the containment vessel during a LOCA are collected by the sump strainers. The sump strainers prevent debris from flowing into the downstream system which includes the reactor core; however, some of the debris may bypass the sump strainers and ultimately reach the reactor core. Due to this possibility, the effect of downstream debris build-up on long term core cooling needs to be determined.

The intent of this technical report is to assess the long-term core coolability of the US-APWR in the event of a LOCA, assuming downstream debris build up within a fuel assembly.

A series of core inlet blockage tests were performed to obtain pressure drop data through a debris laden US-APWR fuel assembly mock-up with half-gap size between the fuel assembly and its housing under debris conditions reflecting design changes in ECC recirculation water return path to refueling water storage pit (RWSP). The tests attempt to demonstrate that downstream core debris build up does not block adequate long-term cooling flows from reaching the core.

Seven (7) tests were performed by varying the parameters according to break location and particulate to fiber ratio (P/F). The acceptance criterion of the assembly head loss caused by debris accumulation was identified for each case and confirmed to satisfy the US-APWR design.

The test results for the expected amount of debris show that sufficient driving head is available in order to generate adequate flow for decay heat removal during post-LOCA recirculation. Thus, core coolability is maintained in the event of downstream debris build up.

Table of Contents

Table of Contents ..... **iii**
List of Tables ..... **v**
List of Figures ..... **vi**
List of Acronyms ..... **vii**
1.0 INTRODUCTION **1**
2.0 OBJECTIVE **2**
3.0 TEST PLAN **3**
3.1 Post-LOCA Conditions 3
3.1.1 Hot Leg Break 3
3.1.2 Cold Leg Break 3
3.1.3 Cold Break after Hot Leg Switch Over 4
3.2 Acceptance Criteria for the Pressure Drop 4
3.3 Test Description 4
3.4 Scaling 5
3.5 QA Program 5
4.0 TEST FACILITY **9**
4.1 Test Loop 9
4.2 Test Section and Mock-Up Assembly 9
4.3 Measurement System 10
5.0 TEST CONDITION **16**
5.1 Flow Rate 16
5.2 Debris 17
5.2.1 Non-Chemical Debris 17
5.2.2 Chemical Debris 18
5.2.3 Test Debris Quantity 18
5.3 Test Matrix 20
6.0 TEST PROCEDURE AND EVALUATION METHOD **22**
6.1 Test Procedure 22
6.2 Data Processing 22
6.3 Evaluation Method 23
6.4 Repeatability 23
7.0 TEST RESULTS **25**
7.1 Hot Leg Break Tests 25
7.1.1 Summary of Hot Leg Break Tests 25
7.1.2 HL1-h2 26
7.1.3 HL2-h2 30
7.1.4 HL3-h2 34
7.1.5 Results of Hot Leg Break Tests 38
7.2 Cold Leg Break Tests 39
7.2.1 Summary of Cold Leg Break Tests 39
7.2.2 CL1-h2 40
7.2.3 CL2-h2 44
7.2.4 CL3-h2 48
7.2.5 Results of Cold Leg Break Tests 52
7.3 Cold Leg Break after HLSO Test 53
7.3.1 CL(HLSO)-h2 53
7.3.2 Results of Cold Leg Break after HLSO Test 57
8.0 CONCLUSION **58**

9.0 REFERENCES 59
Appendix-A Non-Chemical Debris Preparation 60
Appendix-B Chemical Debris Preparation 62

List of Tables

Table 3.5-1 Representative post-LOCA conditions 6
Table 3.5-2 Summary of acceptance criteria 6
Table 4.3-1 Accuracy of the measurement instruments 11
Table 5.1-1 Flow rate conditions 16
Table 5.2-1 Debris types and quantities 19
Table 5.2-2 Test condition of debris quantities 19
Table 5.3-1 Test matrix 21
Table 7.1-1 Test parameters for HL1-h2 27
Table 7.1-2 Test sequence of HL1-h2 27
Table 7.1-3 Test parameters for HL2-h2 31
Table 7.1-4 Test sequence of HL2-h2 31
Table 7.1-5 Test parameters for HL3-h2 35
Table 7.1-6 Test sequence of HL3-h2 35
Table 7.2-1 Test parameter for CL1-h2 41
Table 7.2-2 Test sequence of CL1-h2 41
Table 7.2-3 Test parameter for CL2-h2 45
Table 7.2-4 Test sequence of CL2-h2 45
Table 7.2-5 Test parameter for CL3-h2 49
Table 7.2-6 Test sequence of CL3-h2 49
Table 7.3-1 Test parameter for CL(HLSO)-h2 54
Table 7.3-2 Test sequence of CL(HLSO)-h2 54

List of Figures

Figure 3.5-1 Illustration of the Post-LOCA Conditions 7
Figure 3.5-2 Comparison of the mock-up and full-scale assembly 8
Figure 4.3-1 Schematic diagram of the test loop 11
Figure 4.3-2 Test loop for CIB test 12
Figure 4.3-3 Test section and measurement position 13
Figure 4.3-4 Half-gap size of test section 14
Figure 4.3-5 Schematic diagram of measurement system 15
Figure 6.4-1 Overview of test procedure 24
Figure 7.1-1 Calculated differential pressure vs. Particle/Fiber ratio on Additional HL tests 25
Figure 7.1-2 Time sequence data of HL1-h2 28
Figure 7.1-3 Photographs of the mock-up assembly after HL1-h2 29
Figure 7.1-4 Time sequence data of HL2-h2 32
Figure 7.1-5 Photographs of the mock-up assembly after HL2-h2 33
Figure 7.1-6 Time sequence data of HL3-h2 36
Figure 7.1-7 Photographs of the mock-up assembly after HL3-h2 37
Figure 7.2-1 Calculated differential pressure vs. Particle/Fiber ratio on Additional CL Tests 39
Figure 7.2-2 Time sequence data of CL1-h2 42
Figure 7.2-3 Photographs of the mock-up assembly after CL1-h2 43
Figure 7.2-4 Time sequence data of CL2-h2 46
Figure 7.2-5 Photographs of the mock-up assembly after CL2-h2 47
Figure 7.2-6 Time sequence data of CL3-h2 50
Figure 7.2-7 Photographs of the mock-up assembly after CL3-h2 51
Figure 7.3-1 Time sequence data of CL(HLSO)-h2 55
Figure 7.3-2 Photographs of the mock-up assembly after CL(HLSO)-h2 56

List of Acronyms

Alion	Alion Science and Technology
CIB	Core Inlet Blockage
CL	Cold Leg
CV	Containment Vessel
DP	Differential Pressure
DVI	Direct Vessel Injection
ECCS	Emergency Core Cooling System
FA	Fuel Assembly
HL	Hot Leg
HLSO	Hot Leg Switch Over
LDFG	Low Density Fiberglass
LOCA	Loss Of Coolant Accident
LTCC	Long Term Core Cooling
MHI	Mitsubishi Heavy Industries, Ltd.
PCI	Performance Contracting Incorporated
RWSP	Refueling Water Storage Pit
R&D	Research and Development
SG	Steam Generator
SI	Safety Injection

1.0 INTRODUCTION

This report presents the core inlet blockage test description and results conducted by Mitsubishi Heavy industries Ltd. (MHI), in response to Generic Safety Issue 191 (GSI-191).

GL 2004-02 (Ref.1.0-1) requests that licensees address the effects of downstream debris build-up on post-LOCA long-term core cooling (LTCC). In order to address the plant-specific aspects of this subject, MHI issued a technical report “US-APWR Sump Strainer Downstream Effects.” (Ref. 1.0-2)

The technical report assesses the US-APWR systems and components downstream of the containment sump strainers to ensure that these systems and components operate as designed under post-LOCA conditions. The report incorporates lessons learned and best practices from GSI-191 and GL 2004-02. It was prepared in accordance with NEI 04-07 and published NRC staff expectations. The report also meets the intent of previous industrial studies in the U.S. as adapted for the US-APWR design. The report concludes that operation under post-LOCA conditions with debris-laden fluid will not result in a flow rate below that required for LTCC because the US-APWR is a low fiber plant equipped with high performance strainers. Fuel cladding temperatures will remain below those required by 10CFR50.46.

The purpose of the series of tests is to supplement the technical reports (Ref.1.0-2 and 3) and to provide the NRC with additional supporting information. The testing was performed at MHI Takasago R&D Center.

The test facility comprises a US-APWR fuel assembly mock-up with half-gap size between fuel assembly and its housing. Further, in evaluation of the amount of debris to be applied to the tests, MHI has applied 1) a bypass ratio supported by bypass fiber test result (Ref.1.0-2 Appendix-J), 2) and a reduction based on core bypass flow with the DVI to hot-leg switch over time for cold-leg break (Ref.1.0-2 Appendix-I).

Also, the test conditions incorporated an increase in chemical debris loading, which stems from a design change of ECC recirculation water flow path to RWSP. Additional core inlet blockage tests are needed due to these changes resulting in an increase in chemical debris loading. This report provides results of the core inlet blockage test for the US-APWR.

2.0 OBJECTIVE

The objective of the core inlet blockage test is to obtain pressure drop data through an US-APWR fuel assembly mock-up that simulates debris build-up. The data will be used to demonstrate that sufficient driving head is available to maintain adequate flow to remove decay heat during post-LOCA recirculation in the event of fuel assembly debris build up. This will provide the NRC with confirmation that Long Term Core Coolability is adequately maintained in the US-APWR.

3.0 TEST PLAN

3.1 Post-LOCA Conditions

Post-LOCA conditions under LTCC are represented by three state points summarized in Table 3.5-1. These state points are selected based on the break location and operation mode that affect core flow rate, flow direction and driving force. The core flow rate and flow direction is considered to affect debris behavior, and the break location determines the driving force that generates the core flow. As shown in Table 3.5-1, these state points cover the minimum and maximum of the core flow rate and flow direction in the core during LTCC given the different break locations. Therefore, these state points adequately represent possible flow patterns in the core during LTCC. Illustrations of the state points are shown in Figure 3.5-1. Detailed description of the state points is given in the following subsections.

3.1.1 Hot Leg Break

When a LOCA occurs, the emergency core cooling system (ECCS) injects water through direct vessel injection (DVI) nozzles. If the break location is in the hot leg (HL), all the ECCS injected water will pass through the reactor core before spilling out from the break location. Therefore, the core flow rate is assumed to be equal to the flow rate of the four safety injection (SI) pumps. This assumption represents the maximum possible flow rate during LTCC. If the core pressure drop increases due to debris build-up, the water level in the steam generator (SG) tubes rise to meet the pressure increase at the injection point until it reaches the top of the SG tube. In this case, the maximum available driving force for the core flow is the difference in the hydraulic head between the top of the SG tube and the core water level. The void fraction in the core is conservatively neglected.

The SI flow rate is assumed to be conservative because the pressure drop becomes higher as the flow rate increases, whereas the maximum available driving force is constant irrespective of the number of SI pumps in operation. This is due to the fact that a single SI pump is able to generate sufficient hydraulic head to raise the water level to the top of the SG tube. Therefore, the total flow rate out of all four SI pumps is chosen as a representative condition for HL break.

3.1.2 Cold Leg Break

If the break location is in the cold leg (CL), a large portion of injected water spills out from the break point because the DVI nozzles are located close to the CL and sufficient driving force to inject all the water against core pressure is not available. As a consequence, only a small portion of the water from the ECCS flows through the core. Core cooling is an issue as the water in the core boils off due to the decay heat. Therefore, the core flow rate needs to be sufficient to compensate for core boil off such that the core can remain covered. The driving force of the core flow is determined by the water level in the CL piping and the core water level. For the core water level, a collapsed water level that considers void fraction is used. This assumption is still conservative because the void fraction considered here is much smaller than the actual void fraction.

The driving force of the core flow is not affected by SI flow rate because any redundant SI water flow greater than the boil off flow rate will spill out from the break point and water level in the CL piping will be maintained during LTCC, as mentioned above.

3.1.3 Cold Break after Hot Leg Switch Over

The US-APWR is designed so that the ECCS injection mode changes from DVI injection mode to simultaneous DVI nozzle and HL injection mode four hours after the LOCA occurs, which is called hot leg switch over (HLSO). In this operation mode, two of the four SI pumps inject water through DVI nozzles and the remaining two inject from the HL. When the break location is in the CL, a large portion of the injected water from the DVI nozzles spills out from the break location in a similar manner to the cold leg break, and the core flow is dominated by the injection through the HL. Therefore, the flow rate is assumed to be the flow rate of two SI pumps. At the same time, the pressure at the injection point can increase until the water level reaches the top of the SG tube as in the case of the HL break. The driving force is then defined as the hydraulic head between the top of the SG tube and the water level in the CL piping.

3.2 Acceptance Criteria for the Pressure Drop

In order to maintain the LTCC, the acceptance criteria ($DP_{available}$) for the pressure drop due to the debris bed build-up are defined in relation to a maximum available driving force ($DP_{drivingforce}$).

As described in the previous section, $DP_{drivingforce}$ is determined by break location and operation mode. $DP_{available}$ is calculated from the following equation (1), where DP_{flow} is pressure drop over the entire flow loop (primary circulation system and the core) evaluated based on the specified flow rate for each state point.

$$DP_{available}. = DP_{drivingforce} – DP_{flow} \qquad (1)$$

The acceptance criteria are $DP_{available}$. The acceptance criteria are compared against the calculated DP, which is the pressure drop over full scale fuel assembly calculated from the test data as described in Section 6.3.

$$DP_{available} > \text{Calculated DP} \qquad (2)$$

$DP_{available}$ depends on the state points, and Table 3.5-2 summarizes the acceptance criteria for each state point for the US-APWR.

Details on the method of defining the acceptance criteria for each state are described in Appendices H and J of MUAP-08013 (Ref.1.0-2).

3.3 Test Description

In order to demonstrate the acceptance criteria mentioned above are met during the post-LOCA recirculation, the core inlet blockage test was conducted. The test utilized a single mock-up assembly contained in a test section as a representative of the US-APWR core, and the post-LOCA debris laden flow was simulated by introducing three types of debris: particulate, fibrous and chemical debris. Pressure drop over the several segments of the mock-up assembly was measured to determine the pressure drop increase due to the debris accumulation. The test is performed using room temperature water under atmospheric pressure. The flow rate is selected as 1/257 of the US-APWR core flow rate of corresponding scenario so that the flow rate through the mock-up assembly is identical to that through the

fuel assembly in the US-APWR core. The amount of debris is also determined as 1/257 of the postulated amount in the US-APWR core.

3.4 Scaling

As described in the previous section, the test utilizes a single mock-up assembly to represent the US-APWR core. Therefore, flow rate and amount of debris are scaled as 1/257 of the postulated amount in the actual plant. The other issues where the scaling is involved are the fuel length, number of grid spacers of the test assembly, and flow conditions at room temperature under atmospheric pressure, which are elaborated as follows.

The mock-up assembly is considered as a conservative representation of the full-scale fuel assembly when appropriate scaling is applied. In the core inlet blockage test, the upstream grid spacers generally collect larger amount of debris because the concentration of debris in the upstream flow is larger. Therefore, the pressure drop over the downstream grid spacers can be conservatively substituted with the pressure drop over the upstream grid spacers.
[

]

The use of room temperature fluid conservatively covers the post-LOCA core condition because the high kinematic viscosity of the room temperature fluid yields low Reynolds number flow when identical flow rate is assumed. The low Reynolds number flow yields a generally higher pressure drop coefficient. In addition, the dynamic pressure is larger at lower temperature due to the temperature dependence of the water density. Therefore, the evaluation of the pressure drop coefficient at room temperature is conservative.

In the post-LOCA core condition where the LTCC is an issue, the pressure will approach the atmospheric pressure when a large break LOCA that would generate large amount of debris is considered. Furthermore, there is little effect of system pressure for the test. Therefore, the use of atmospheric pressure in the test is considered to be valid.

3.5 QA Program

The core inlet blockage test was performed under the quality assurance program of MHI Takasago R&D Center that satisfies the requirements of Appendix-B to 10 CFR Part 50 and 10 CFR Part 21, which has been approved by MHI Nuclear Energy Systems Quality and Safety Management Department.

Table 3.5-1 Representative post-LOCA conditions

Break Location	Operation Mode	Flow rate	Core Flow Direction
HL	Direct vessel injection (DVI)	Maximum for 4 SI pumps	Upward
CL	DVI	Minimum required	Upward
CL	DVI and hot leg injection	Maximum for 2 SI pumps	Downward

Table 3.5-2 Summary of acceptance criteria

	Driving force	Flow rate	Acceptance criteria
HL break	Water level between HL pipe and top of the shortest SG tube	Maximum Flow rate	[ ] [ ]
CL break	Water level between CL pipe and core collapsed considering core boiling	Minimum Flow rate (Boil off flow rate)	[ ] [ ]
CL break after HLSO	Water level between CL pipe and top of the shortest SG tube	Maximum Flow rate	[ ] [ ]

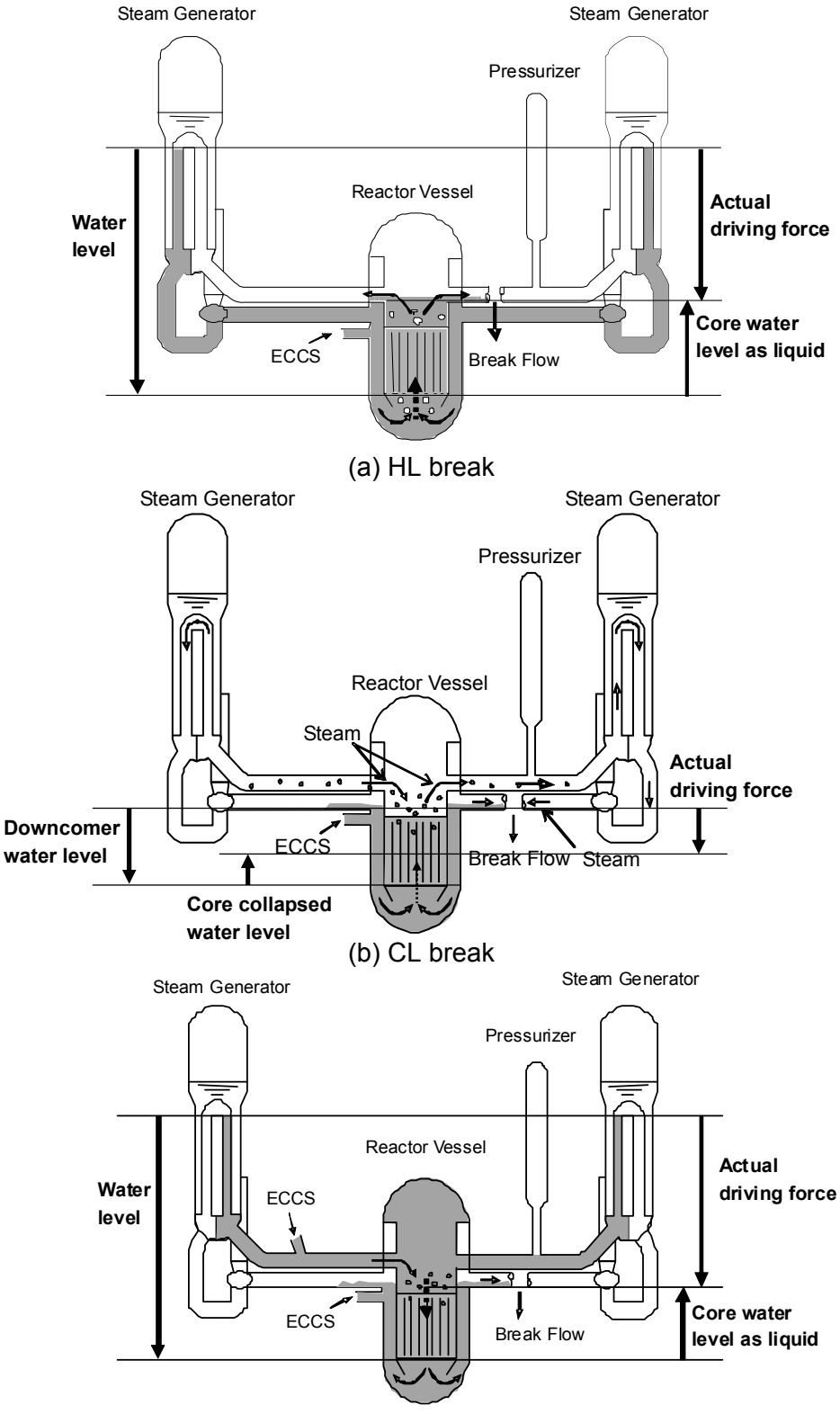

Figure 3.5-1 Illustration of the Post-LOCA Conditions

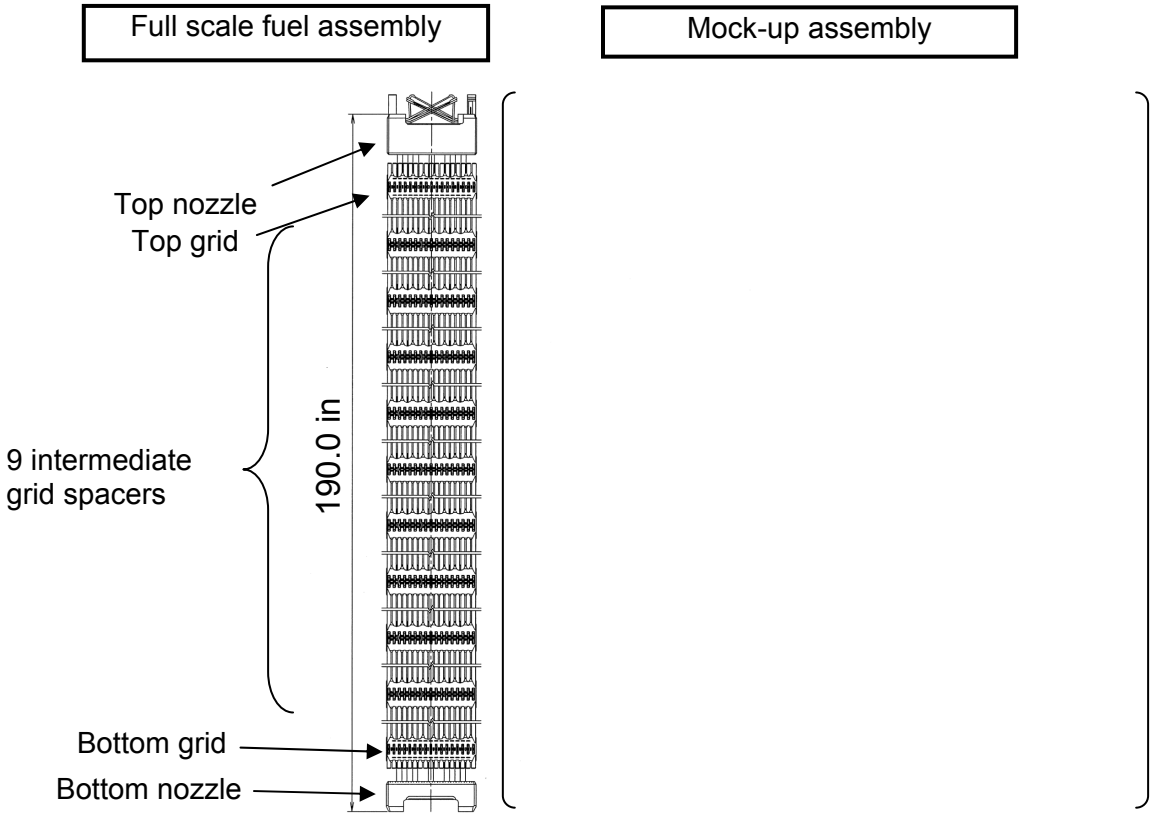

Figure 3.5-2 Comparison of the mock-up and full-scale assembly

4.0 TEST FACILITY

The test facility has been constructed at MHI Takasago R&D Center in Japan. A description of the test loop is given in Section 4.1. A detail of the mock-up assembly is described in Section 4.2, and Section 4.3 describes the measurement system.

4.1 Test Loop

The test loop consists of a test section, a reservoir tank and circulation system. A schematic diagram is shown in Figure 4.3-1, and a photograph of the test loop is shown in Figure 4.3-2.

The test section is made of transparent acrylic plates, which enables visual observation during the tests. The flow direction through the test section can be changed by valves, so that either a forward or backward flow mode can be selected.

The reservoir tank is a plastic tank. Debris is injected in this tank during the tests and the fluid in this tank is continuously stirred with an agitator to have homogenized debris/water mixture. The tank has a conical bottom to avoid debris precipitation on the bottom.

Simulating [ ] inlet flow holes in the lower core support plate per fuel assembly, the circulation system has [ ] separate lines at the inlet of the test section. Each line is equipped with a circulation pump and connected to [ ] holes of the lower core support plate through a conical diffuser. For simplicity, only one line is shown in Figure 4.3-1. The circulation pumps generate constant volumetric flow rate for the solid-liquid mixture by controlling rotation speed. The flow rate of each line is measured at the inlet of the test section with an electromagnetic flow meter, and feedback control is applied to the circulation pumps. This enables separate control of the flow rate through the [ ] holes of the lower core support plate. Flow rates of the [ ] lines are carefully controlled, so that uniform flow rate at the core inlet is achieved. In addition, direct connections of the tubes to the holes of the core support plate ensure all the debris in the system is introduced to the core. This realizes a very conservative assumption considering that the debris could precipitate in the lower plenum in the actual plant

4.2 Test Section and Mock-Up Assembly

The test section contains a mock-up assembly which simulates the US-APWR fuel assembly. The mock-up assembly is braced with a simulated lower core support plate and upper core plate. A comparison of the mock-up assembly with the full length US-APWR fuel is shown in Figure 3.5-2. The mock-up assembly is comprised of 17×17 fuel rods supported by [ ] grid spacers and has the equivalent configuration to the US-APWR fuel assembly except that the length is approximately [ ] The top and bottom Inconel grid spacers have no mixing vanes, which is also equivalent to the US-APWR fuel assembly. [
] whereas the nine intermediate grid spacers of the US-APWR fuel have mixing vanes.

The test section was equipped with pressure taps as shown in Figure 4.3-3, and the differential pressure between specified combinations of the pressure taps were transformed to voltage signal by pressure transducers (digital manometers). In each vertical position, there are [ ] pressure taps in the circumferential direction, and these pressure taps are connected to each other with pressure conduit so that the pressure is equalized and average pressure

can be measured. As shown in Figure 4.3-4, the test section is modified to the half-gap size in actual core between a fuel assembly and wall for conservative simulation of an actual plant.

4.3 Measurement System

In the core inlet blockage test, differential pressure over the test assembly is measured. Water temperature and flow rate are also measured and monitored during the test. Figure 4.3-5 shows a schematic diagram of the measurement system. All the data is collected and stored in the data acquisition computer via analog input module.

Four types of digital manometers, whose ranges are 1 kPa, 10 kPa, 130 kPa and 500 kPa, respectively, are used in parallel in order to cover the possible range of differential pressure. Figure 4.3-3 shows [ ] combinations of the pressure taps with which pressure measurements are performed. A single set of manometers is used to measure all the measurement positions by connecting the pressure conduit in parallel and being switched with actuated ball valves. [

]

The water temperature is measured with a thermocouple in the return line. The data is continuously monitored and recorded in the data acquisition computer.

The flow rate in [ ] circulation lines at test section inlet is measured with [ ] electromagnetic flow meters installed in each line. The piping upstream of the flow meter has 10 times the pipe diameter of the straight section so as to measure the flow rate with sufficient accuracy. The measured flow rate is used for controlling the pump speed via feedback control system.

Measurement accuracy of the instruments is summarized in Table 4.3-1. All the instruments are calibrated before and after the all tests. The integrity of the flow loop and measurement system is confirmed by differential pressure measurements without debris before each test run.

Table 4.3-1 Accuracy of the measurement instruments

Instruments	Accuracy
Thermocouple	[ ]
Digital manometer	[ ]
Flow meter	[ ] [ ]

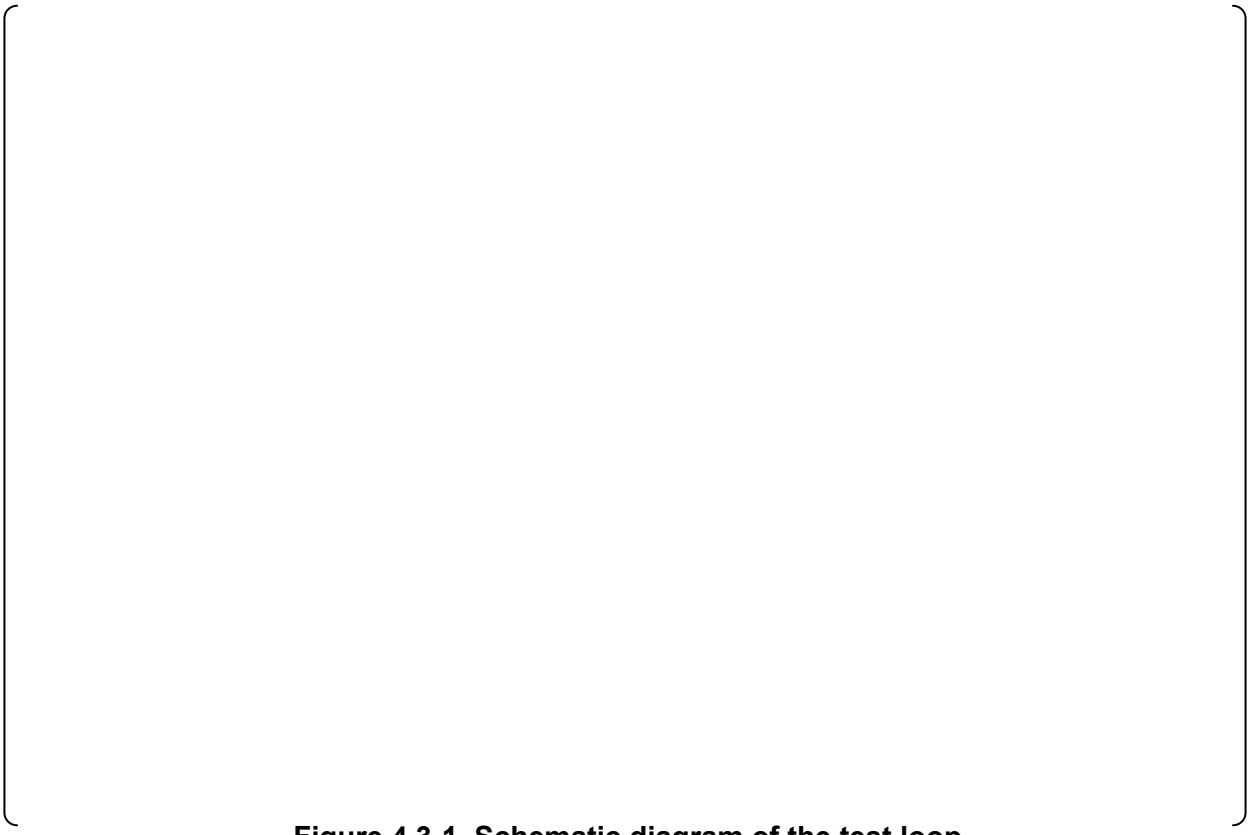

Figure 4.3-1 Schematic diagram of the test loop

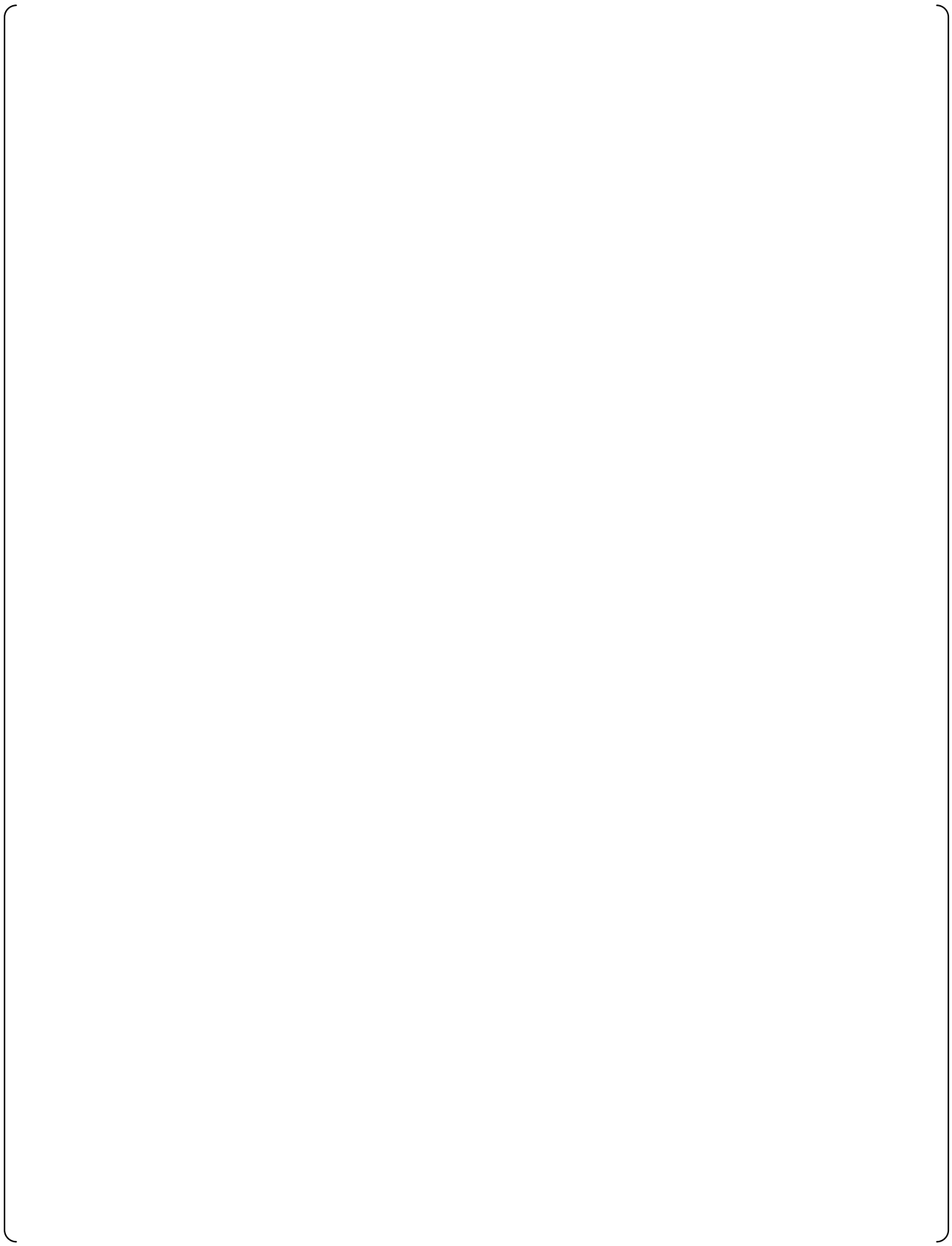

Figure 4.3-2 Test loop for CIB test

Figure 4.3-3 Test section and measurement position

Figure 4.3-4 Half-gap size of test section

Figure 4.3-5 Schematic diagram of measurement system

5.0 TEST CONDITION

5.1 Flow Rate

The flow rates in Table 5.1-1 are selected as bounding conditions that cover possible core flow rates in the post-LOCA core conditions. The flow direction is either forward (upward direction in the core) or backward (downward direction in the core) depending on the post-LOCA injection mode. Underlying ideas are addressed in section 3.1. The flow rates are determined as 1/257 of the actual US-APWR core flow rate.

The flow rate for the HL break cases is the maximum flow rate in the forward direction that occurs during the hot leg break. This flow rate is determined as the combined flow rate of four SI pumps.

The flow rate for the CL break cases is the flow rate that meets the boil-off flow rate to maintain the core covered with the coolant. This represents the lower bound of the possible flow rate during the post-LOCA recirculation.

The CL break after HLSO represents the maximum flow rate in the backward direction that occurs during the CL break after HLSO. The flow rate in this case is determined as the flow rate of the two SI pumps.

Details on the method of defining the flow rate for each break position are described in Appendices H and J of MUAP-08013 (Ref.1.0-2).

Table 5.1-1 Flow rate conditions

Scenario	Flow direction	US-APWR Flow Rate	Test Flow Rate *1	Remarks
HL Break	Forward	5848 gpm	22.8 gpm	Max. safeguard flow rate of Four(4) SI pumps
CL Break	Forward	907 gpm	3.5 gpm	Boil off flow rate at 850s*2
CL Break after HLSO	Backward	2924 gpm	11.4 gpm	Max. safeguard flow rate of two(2) SI pumps

*1: 1/257 of the flow rate for the US-APWR
*2: Ref 1.0-2 Appendix E

5.2 Debris

All debris used for the test is prepared and is consistent with the design basis debris characteristics of the US-APWR discussed in Section 3.3 and Table 3.5-1, and Appendix-C of MUAP-08001 “Sump Strainer Performance” (Ref.1.0-3). The characteristics of non-chemical debris and chemical debris are discussed in following subsections 5.2.1 and subsection 5.2.2 respectively, and summarized in Table 5.2-1 and Table 5.2-2. The debris preparation procedures are discussed in Appendix-A and B.

5.2.1 Non-Chemical Debris

5.2.2 Chemical Debris

5.2.3 Test Debris Quantity

The quantity of debris used for the core inlet blockage test is a combination of two factors: first, the quantity of plant debris [ ], and second, the quantity of core bypass debris [ ]. Detail of these two factors are described below, and the conclusive debris amount used for the CIB testing is summarized in Table 5.2-1 and Table 5.2-2.

Table 5.2-1 Debris types and quantities

Table 5.2-2 Test condition of debris quantities

5.3 Test Matrix

The test matrix is shown in Table 5.3-1. The debris condition for the tests is shown in Table 5.2-2. For the HL break tests and CL break tests, the ratio of the particulate to fibrous debris was considered as a variable parameter. For CL(HLSO), the test was only performed with the debris condition.

In the HL break tests, the first case (HL1-h2) was chosen to be the particulate to fibrous ratio of [ ] which consists of both of the [ ] amount of particle debris and the [ ] amount of fiber debris. The third case (HL3-h2) was chosen to be the [ ] in order to confirm the trend of the particulate to fibrous ratio in the HL break tests. The second case (HL2-h2) was chosen to be the [ ] in order to confirm the trend of the particulate to fibrous ratio in the HL break tests.

In the CL break tests, the first case (CL1-h2) was chosen to be the particulate to fibrous ratio of [ ] which consists of the [ ] amount of particle debris and the [ ] amount of fiber debris. The third case (CL3-h2) was chosen to be the particulate to fibrous ratio of [ ]. The second case (CL2-h2) was chosen to be the [ ] in order to confirm the trend of the particulate to fibrous ratio in the CL break tests.

Table 5.3-1 Test matrix

Case	Particle/Fiber ratio	Fibrous debris	Particulate debris	Chemical debris	Flow rate
HL1-h2	[ ]	[ ]	[ ]	[ ]	22.8 gpm (86.3 liters/min)
HL2-h2	[ ]		[ ]		
HL3-h2	[ ]		[ ]		
CL1-h2	[ ]	[ ]	[ ]	[ ]	3.5 gpm (13.3 liters/min)
CL2-h2	[ ]		[ ]		
CL3-h2	[ ]		[ ]		
CL(HLSO)-h2	[ ]	[ ]	[ ]	[ ]	11.4 gpm (43.2 liters/min)

6.0 TEST PROCEDURE AND EVALUATION METHOD

Description of the test procedure, especially about the debris introduction procedure is given in Section 6.1. The data processing method is described in Section 6.2. The evaluation method, how to convert measured pressure drop to the one comparable to the acceptance criteria for the actual plant, is given in Section 6.3.

6.1 Test Procedure

An overview of the test procedure is shown in Figure 6.4-1. Initially the test loop is filled with water, and air slug and bubbles are removed from the test loop. The differential pressure with non-debris laden flow is measured to confirm the integrity of the test facility.

[

]

[

]

[

]

After the termination of the measurement, the water in the test loop is drained slowly so that the debris bed accumulated on the nozzles and grid spacers are preserved for visual observation. The photographs of the debris beds are taken during the visual observation.

6.2 Data Processing

Voltage data from the measurement devices is accumulated in the acquisition computer during the test and converted into physical values.

[

]

[

]

6.3 Evaluation Method

The test results are evaluated at the data point where the total measured differential pressure over the mock-up assembly shows its maximum during a single test run. [

] as shown in equation (6-1). This method ensures conservatism as discussed in section 3.4.

[ ] (6-1)

Calculated DP included the uncertainty evaluation.

The evaluation of measurement uncertainties were based on the GUM (Guide to the Expression of Uncertainty in Measurement) which was published by International Organization for Standardization.

6.4 Repeatability

A repeatability test demonstrates a facility's ability to produce the same test results using identical test conditions as shown below.

- Test facility
- Test equipment (pumps, piping, tanks, envelop, instrument system, data acquisition system)
- Mock-up fuel assembly, water, debris(particle, fiber, chemical)
- Test procedure and operator manipulation

The duplication of these conditions ensures that a proper repeatability test is run and that consistent data is output. The details of the previous repeatability test are reported in MUAP-11022 (Ref.6.4-1). Since this report uses the same test conditions as in MUAP-11022 (Ref.6.4-1), repeatability applies to this report as well.

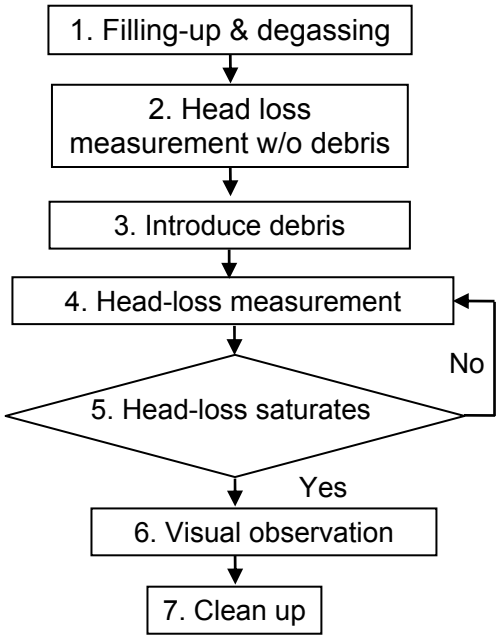

1. Water filling and degassing
2. Measure the head-loss without debris
3. Introduce debris
4. Start the head-loss measurement with debris
5. Continue the measurement until the head-loss saturates
6. Visual observation of the FA is performed after the test
7. The test loop clean-up

Figure 6.4-1 Overview of test procedure

7.0 TEST RESULTS

7.1 Hot Leg Break Tests

7.1.1 Summary of Hot Leg Break Tests

A summary of the HL break test results is shown in Figure 7.1-1, “Calculated DP” is pressure drop over the full scale fuel assembly calculated from the test data. The acceptance criterion is the maximum allowable core pressure drop to ensure the LTCC for the HL break calculated based on the US-APWR design parameters. In all three cases, the calculated differential pressures are less than the acceptance criterion.

Figure 7.1-1 Calculated differential pressure vs. Particle/Fiber ratio on Additional HL tests

7.1.2 HL1-h2

HL1-h2 is the case in [ ]. As a result, the ratio of particulate to fibrous debris is [ ]. The test parameters for HL1-h2 are summarized in Table 7.1-1. The test sequence and corresponding times are shown in Table 7.1-2.

The time sequence data of the differential pressure and flow rate for the HL1-h2 test is shown in Figure 7.1-2. The vertical dotted lines correspond to the time at which debris was added to the loop. The flow rate is well controlled throughout the test. The figure shows that [

]

In the HL1-h2 test, [

]

Photographs of each component of the mock-up assembly were taken after the test and are shown in Figure 7.1-3. The bottom nozzle, bottom grid, 1st intermediated grid, 2nd intermediate grid and top grid were taken from bottom view. The top nozzle was taken from the top view. [

]

Table 7.1-1 Test parameters for HL1-h2

Volumetric flow rate	86.3 liters/min
Particulate debris	SiC: [ ]
	Dirt/Dust Mix: [ ]
Fibrous debris	[ ]
Chemical debris	[ ]
Particle/Fiber ratio	[ ]

Table 7.1-2 Test sequence of HL1-h2

Figure 7.1-2 Time sequence data of HL1-h2

Figure 7.1-3 Photographs of the mock-up assembly after HL1-h2

7.1.3 HL2-h2

HL2-h2 is performed in order to confirm [ ] The amount of particulate debris [ ] The ratio of particulate to fibrous debris was [ ]. The parameters for HL2-h2 are summarized in Table 7.1-3. Test sequence and corresponding times are shown in Table 7.1-4.

The time sequence data of the differential pressure and flow rate for the HL2-h2 test is shown in Figure 7.1-4. The vertical dotted lines correspond to the time at which debris was added to the loop. The flow rate is well controlled throughout the test. [

]

In the HL2-h2 test, [

]

[

]

Photographs of each component of the mock-up assembly are shown in Figure 7.1-5. [

]

Table 7.1-3 Test parameters for HL2-h2

Volumetric flow rate	86.3 liters/min
Particulate debris	SiC: [ ]
	Dirt/Dust Mix: [ ]
Fibrous debris	[ ]
Chemical debris	[ ]
Particle/Fiber ratio	[ ]

Table 7.1-4 Test sequence of HL2-h2

Figure 7.1-4 Time sequence data of HL2-h2

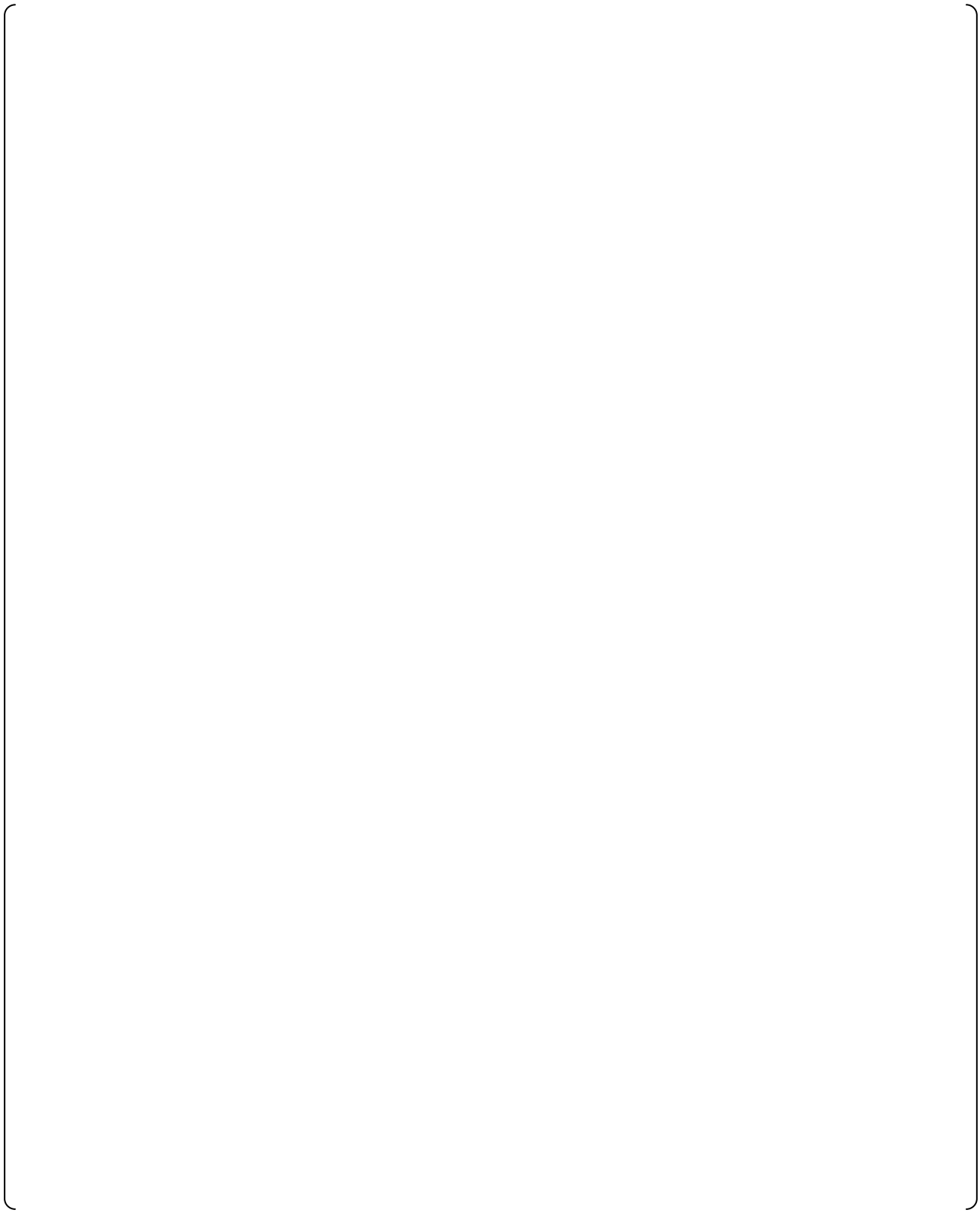

Figure 7.1-5 Photographs of the mock-up assembly after HL2-h2

7.1.4 HL3-h2

HL3-h2 addresses a [ ] particulate to fibrous debris ratio. The quantity of the fibrous debris was assumed to be [ ] and the ratio of particulate to fibrous debris was chosen to be [ ]. The parameters for HL3-h2 are summarized in Table 7.1-5. Test sequence and corresponding times are shown in Table 7.1-6.

The time sequence data of the differential pressure and flow rate for the HL3-h2 test is shown in Figure 7.1-6. The vertical dotted lines correspond to the time at which debris was added to the loop. The flow rate is well controlled throughout the test. The figure shows that [

]

In the HL3-h2 test, [

]

[

]

Photographs of each component of the mock-up assembly are shown in Figure 7.1-7. [

]

Table 7.1-5 Test parameters for HL3-h2

Volumetric flow rate	86.3 liters/min
Particulate debris	SiC: [ ]
	Dirt/Dust Mix: [ ]
Fibrous debris	[ ]
Chemical debris	[ ]
Particle/Fiber ratio	[ ]

Table 7.1-6 Test sequence of HL3-h2

Figure 7.1-6 Time sequence data of HL3-h2

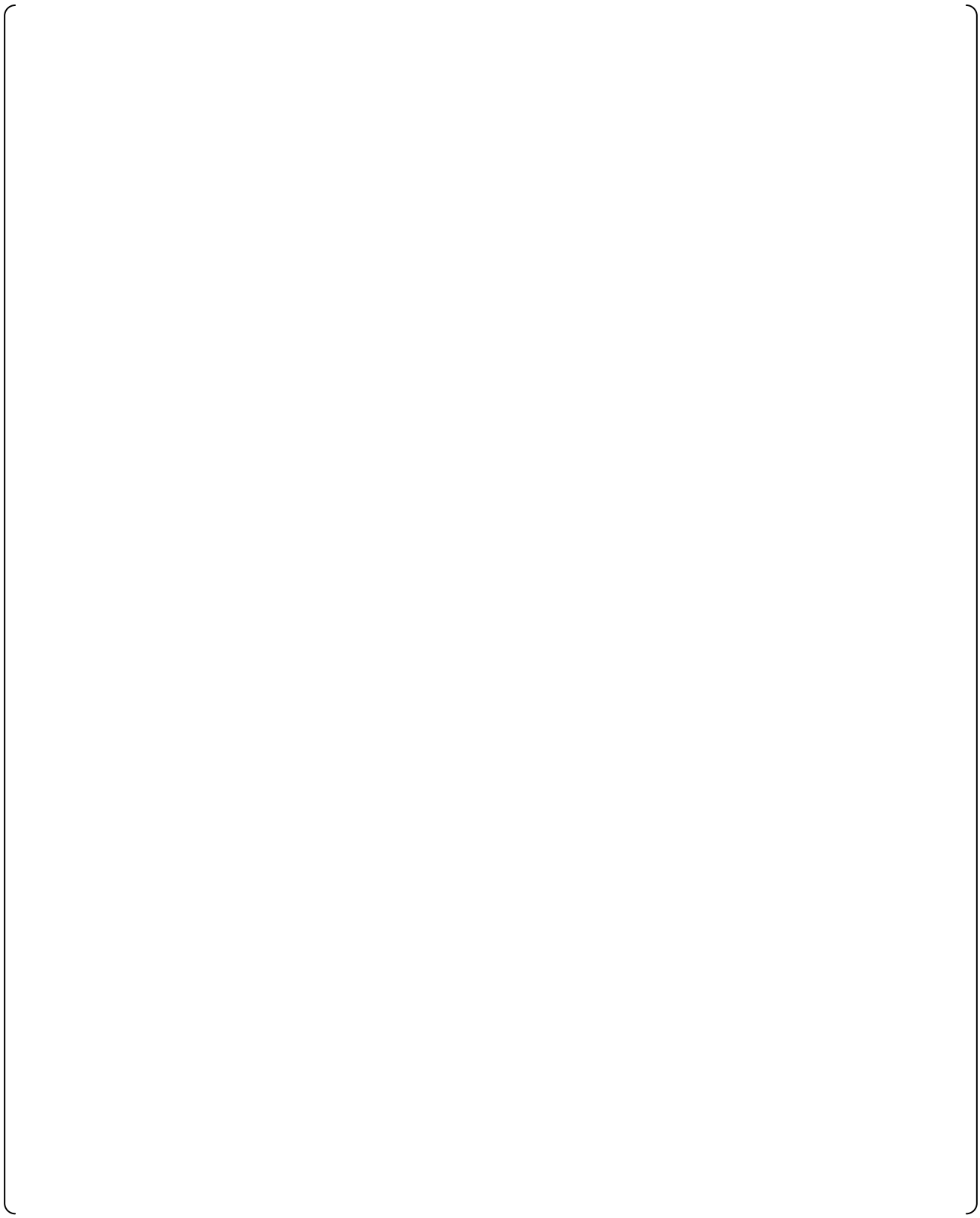

Figure 7.1-7 Photographs of the mock-up assembly after HL3-h2

7.1.5 Results of Hot Leg Break Tests

In order to address the effect of the particulate to fibrous debris ratio, three tests were performed. As shown in Figure 7.1-1, [

]

[

] Even with such conservativeness, the calculated differential pressure is within the acceptable range in the HL break tests.

7.2 Cold Leg Break Tests

7.2.1 Summary of Cold Leg Break Tests

A summary of the CL break test results is shown in Figure 7.2-1. “Calculated DP” is pressure drop over the full-scale fuel assembly calculated from the test data. The acceptance criterion is the maximum allowable core pressure drop to ensure LTCC for the CL break calculated based on the US-APWR design parameters. In all three cases, the calculated differential pressures are less than the acceptance criterion.

Figure 7.2-1 Calculated differential pressure vs. Particle/Fiber ratio on Additional CL Tests

7.2.2 CL1-h2

CL1-h2 is the case in [ ]. As a result, the ratio of particulate to fibrous debris is [ ]. The test parameters for CL1-h are summarized in Table 7.2-1. The test sequence and corresponding time are shown in Table 7.2-2.

The time sequence data of the differential pressure and flow rate for the CL1-h2 test is shown in Figure 7.2-2. The vertical dotted lines correspond to the time at which debris was added to the loop. The flow rate is well controlled throughout the test. [

]

Photographs of each component of the mock-up assembly were taken after the test and are shown in Figure 7.2-3. [

]

Table 7.2-1 Test parameter for CL1-h2

Volumetric flow rate	13.3 liters/min
Particulate debris	SiC: [ ]
	Dirt/Dust Mix: [ ]
Fibrous debris	[ ]
Chemical debris	[ ]
Particle/Fiber ratio	[ ]

Table 7.2-2 Test sequence of CL1-h2

Figure 7.2-2 Time sequence data of CL1-h2

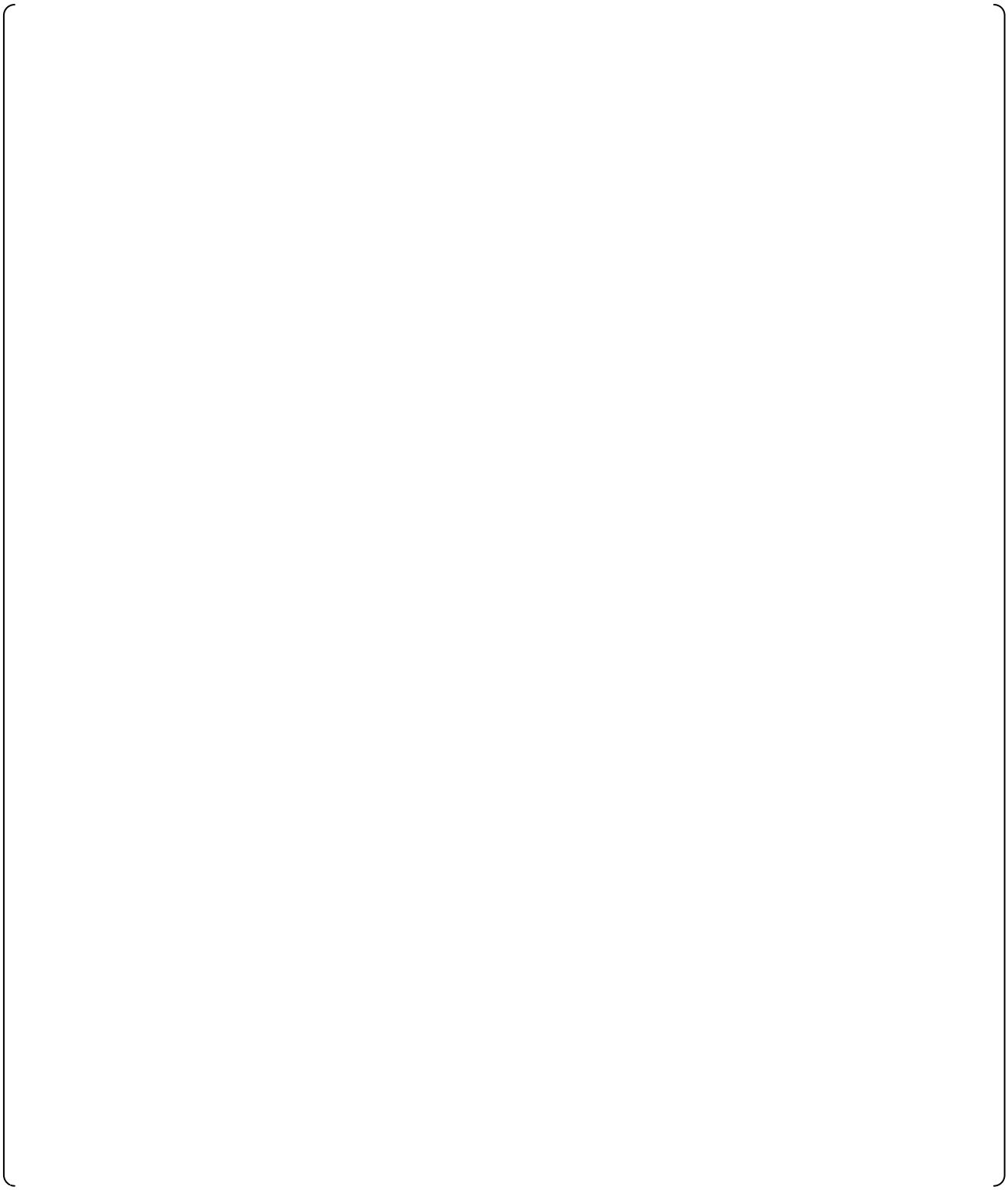

Figure 7.2-3 Photographs of the mock-up assembly after CL1-h2

7.2.3 CL2-h2

CL2-h2 is performed in order to confirm [ ] The amount of particulate debris [ ] The ratio of particulate to fibrous debris was [ ]. The test parameters for CL2-h2 are summarized in Table 7.2-3. The test sequence and corresponding time are shown in Table 7.2-4.

The time sequence data of the differential pressure and flow rate for the CL2-h2 test is shown in Figure 7.2-4. The vertical dotted lines correspond to the time at which debris was added to the loop. The flow rate is well controlled throughout the test. [

]

Photographs of each component of the mock-up assembly were taken after the test and are shown in Figure 7.2-5. [

]

Table 7.2-3 Test parameter for CL2-h2

Volumetric flow rate	13.3 liters/min
Particulate debris	SiC: [ ]
	Dirt/Dust Mix: [ ]
Fibrous debris	[ ]
Chemical debris	[ ]
Particle/Fiber ratio	[ ]

Table 7.2-4 Test sequence of CL2-h2

Figure 7.2-4 Time sequence data of CL2-h2

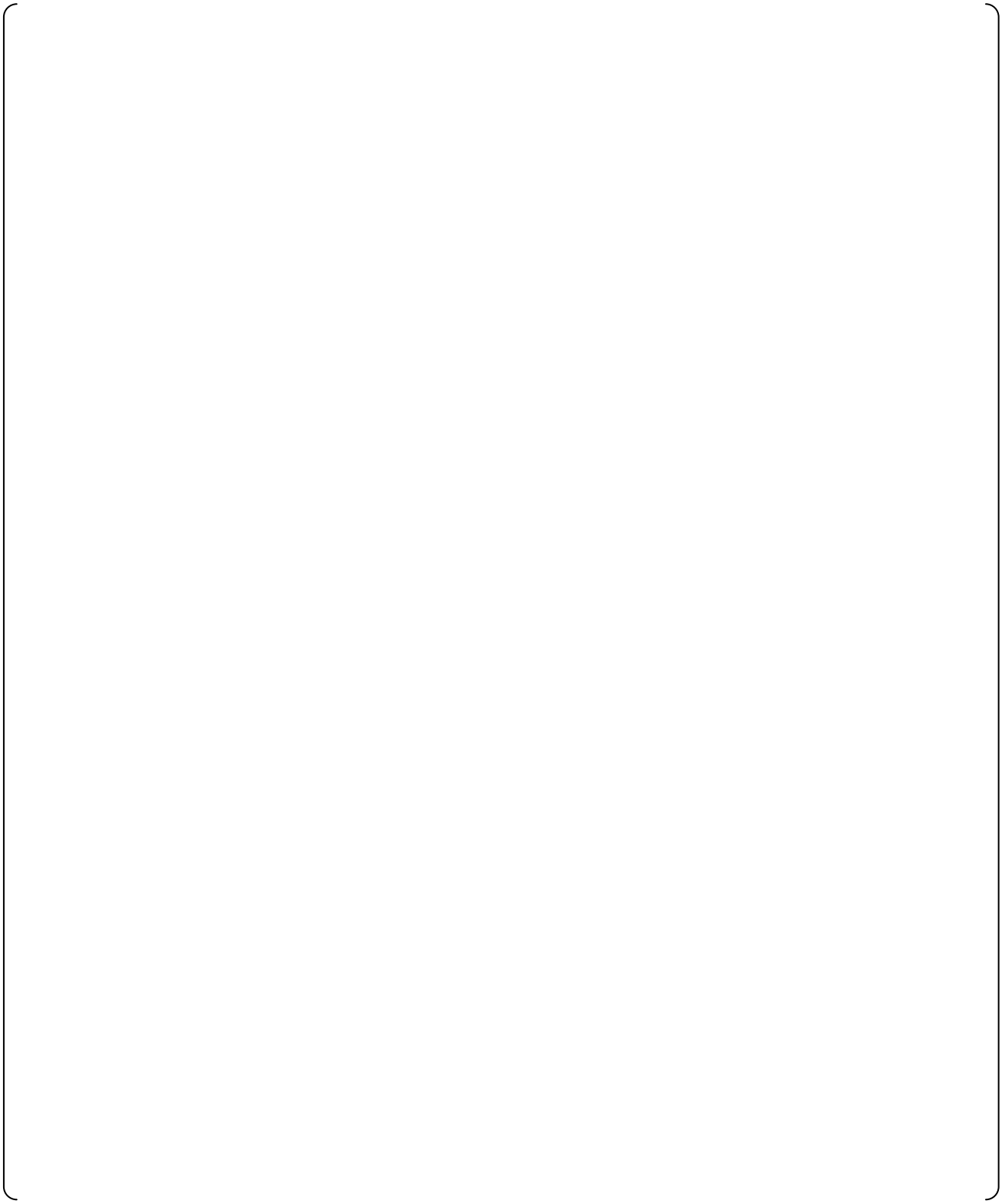

Figure 7.2-5 Photographs of the mock-up assembly after CL2-h2

7.2.4 CL3-h2

CL3-h2 addresses a [ ] particulate to fibrous debris ratio. The quantity of the fibrous debris was assumed to be [ ] and the ratio of particulate to fibrous debris was chosen to be [ ]. The test parameters for CL3-h2 are summarized in Table 7.2-5. The test sequence and corresponding time are shown in Table 7.2-6.

The time sequence data of the differential pressure and flow rate for the CL3-h2 test is shown in Figure 7.2-6. The vertical dotted lines correspond to the time at which debris was added to the loop. The flow rate is well controlled throughout the test. [

]

Photographs of each component of the mock-up assembly were taken after the test and are shown in Figure 7.2-7. [

]

Table 7.2-5 Test parameter for CL3-h2

Volumetric flow rate	13.3 liters/min
Particulate debris	SiC: [ ]
	Dirt/Dust Mix: [ ]
Fibrous debris	[ ]
Chemical debris	[ ]
Particle/Fiber ratio	[ ]

Table 7.2-6 Test sequence of CL3-h2

Figure 7.2-6 Time sequence data of CL3-h2

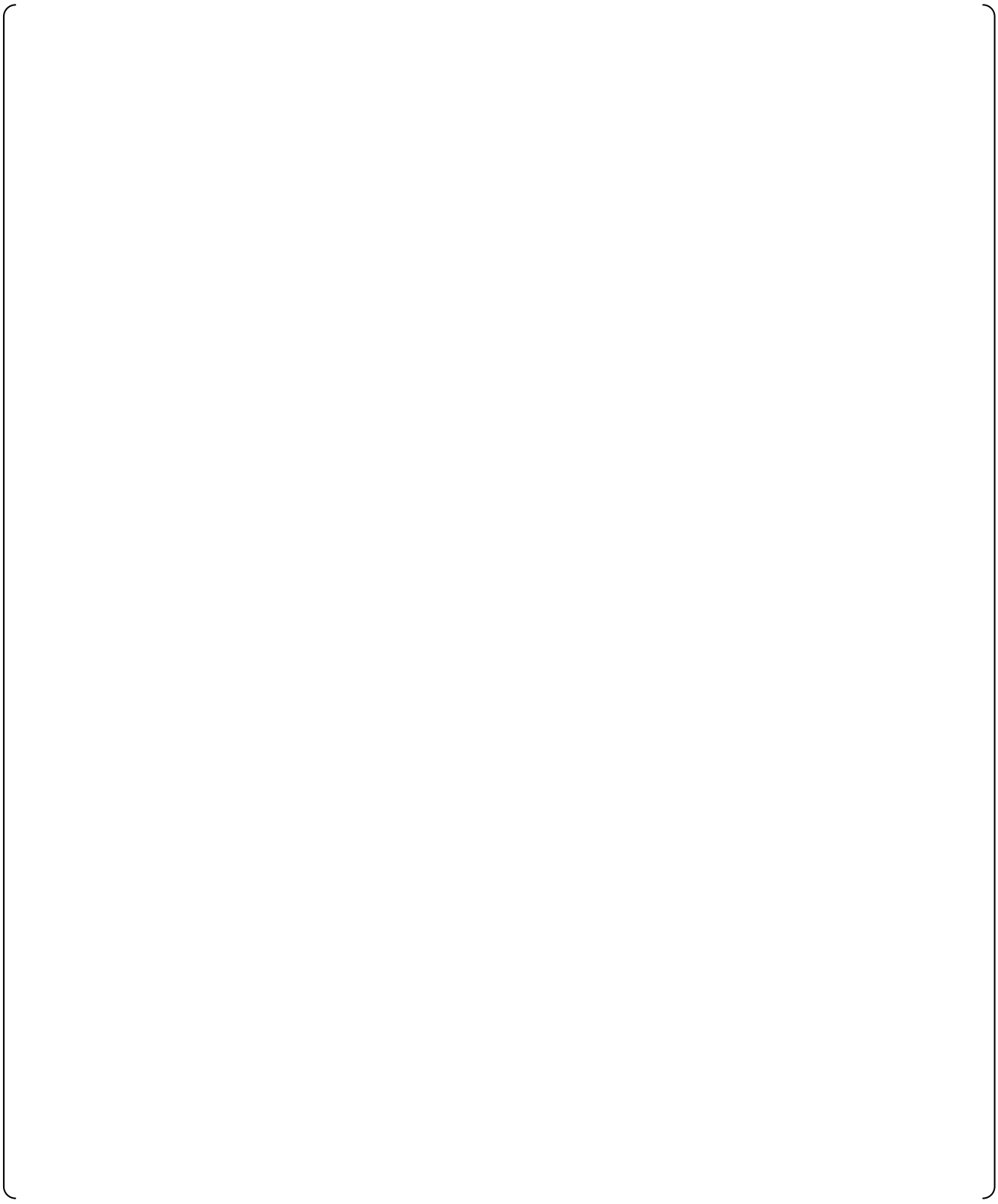

Figure 7.2-7 Photographs of the mock-up assembly after CL3-h2

7.2.5 Results of Cold Leg Break Tests

In order to address the effect of the particulate to fibrous debris ratio and repeatability, three tests were performed. As shown in Figure 7.2-1, [

]

Even with such conservativeness, the calculated differential pressure for the expected amount of debris is within the acceptable range in the CL break tests.

7.3 Cold Leg Break after HLSO Test

7.3.1 CL(HLSO)-h2

CL(HLSO)-h2 is a case in [ ] The ratio of particulate to fibrous debris is [ ]. The test parameters for CL(HLSO)-h2 are summarized in Table 7.3-1. The test sequence and corresponding times are shown in Table 7.3-2.

The time sequence data of the differential pressure and flow rate for the CL(HLSO)-h2 test is shown in Figure 7.3-1. The vertical dotted lines correspond to the time at which debris was added to the loop. The flow rate is well controlled throughout the test. [

]

Photographs of each component of the mock-up assembly were taken after the test and are shown in Figure 7.3-2. Pictures of the grid and nozzle in this figure are taken from the top side of the fuel assembly as the flow direction is from top to bottom of the fuel assembly unlike the other tests. [

]

Table 7.3-1 Test parameter for CL(HLSO)-h2

Volumetric flow rate	43.2 liters/min
Particulate debris	SiC: [ ]
	Dirt/Dust Mix: [ ]
Fibrous debris	[ ]
Chemical debris	[ ]
Particle/Fiber ratio	[ ]

Table 7.3-2 Test sequence of CL(HLSO)-h2

Figure 7.3-1 Time sequence data of CL(HLSO)-h2

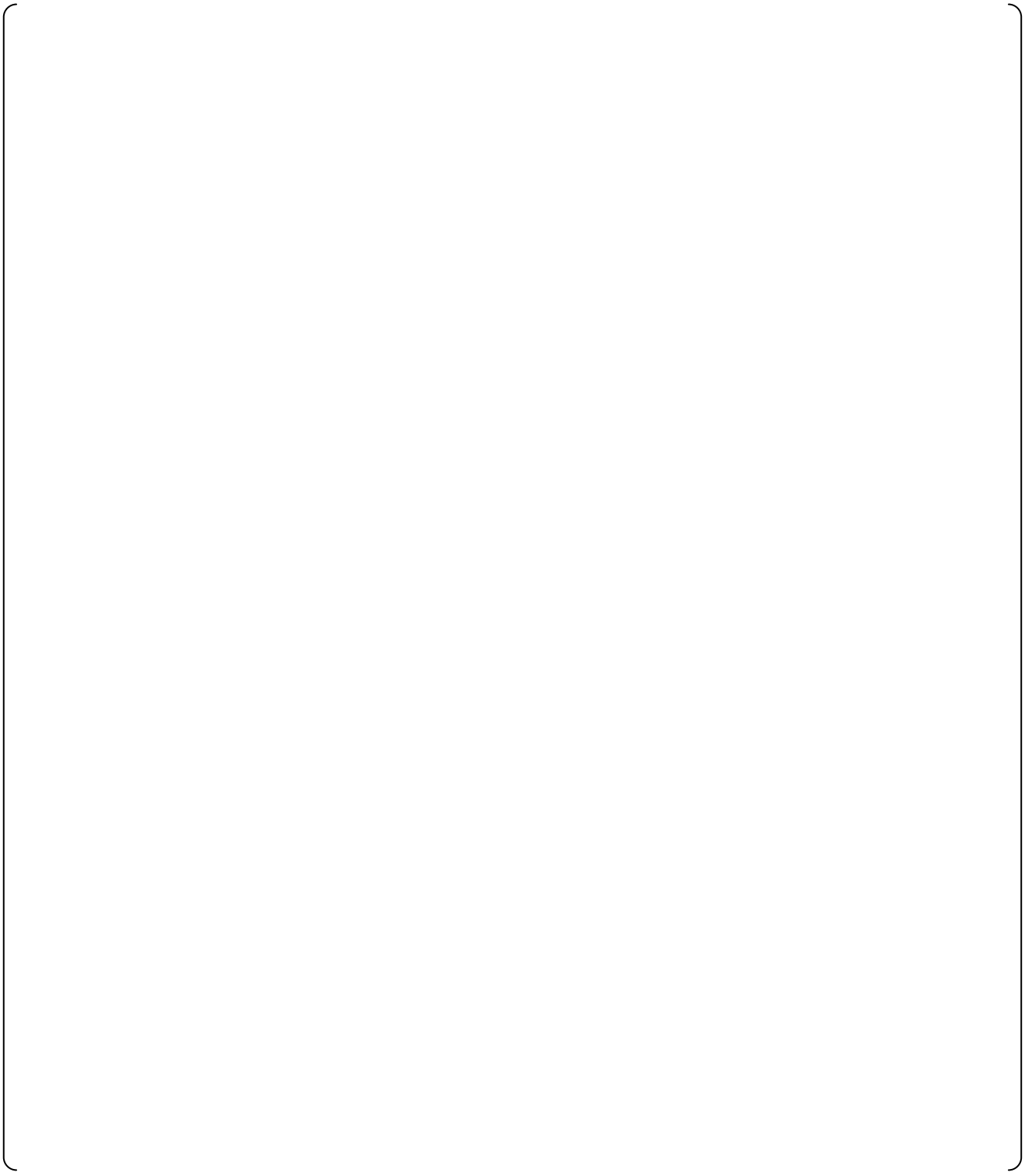

Figure 7.3-2 Photographs of the mock-up assembly after CL(HLSO)-h2

7.3.2 Results of Cold Leg Break after HLSO Test

In the CL break after HLSO, the calculated differential pressure ([ ]) is less than the criterion ([ ]). In this condition, the flow direction is from the top of the mockup fuel assembly to the bottom. [

]

8.0 CONCLUSION

MHI performed the core inlet blockage test with a ratio of the particulate to fibrous debris (P/F) as a parameter for HL break, CL break, and CL break after HLSO cases using half gap.

Seven (7) tests were performed considering break location and P/F ratio as parameters in terms of the effect of debris behavior in the core during LTCC. The acceptance criterion for each combination of break location and ECCS operation mode for the US-APWR design was identified and applied to the tests. The repeatability is also supported by comparison with the test results presented in MUAP-11022 (Ref.6.4-1), which were performed under the same procedure and different amount of the chemical debris.

The test results performed using the design basis amount of debris satisfy the corresponding acceptance criteria, show good repeatability by association with MUAP-11022 (Ref.6.4-1), and demonstrate that sufficient driving head is available to maintain an adequate flow rate to remove decay heat during post-LOCA ECC recirculation with debris laden fluid. Therefore, the test results conclude that the core coolability during LTCC for US-APWR is maintained even if the bypass debris build-up occurs in the core.

9.0 REFERENCES

1.0-1 U.S. Nuclear Regulatory Commission, Potential Impact of Debris Blockage on Emergency Recirculation during Design Basis Accidents at Pressurized Water Reactors, Generic Letter 2004-02, September 2004.

1.0-2 Mitsubishi Heavy Industries, Ltd., US-APWR Sump Strainer Downstream Effects, MUAP-08013-P Revision 5, June 2013.

1.0-3 Mitsubishi Heavy Industries, Ltd., US-APWR Sump Strainer Performance, MUAP-08001-P Revision 8, June 2013.

5.2-1 U.S. Nuclear Regulatory Commission, Characterization and Head-Loss Testing of Latent Debris from Pressurized-Water-Reactor Containment Buildings, NUREG/CR-6877 (LA-UR-04-3970), July 2005.

5.2-2 NRC SE for WCAP-16530-NP-A, Evaluation of Post-Accident Chemical Effects in Containment Sump Fluids to Support GSI-191, TAC No. MD1119, December 21, 2007.

6.4-1 Mitsubishi Heavy Industries, Ltd., US-APWR Additional Core Inlet Blockage Test, MUAP-11022 Revision 1, June 2013.

Appendix-A Non-Chemical Debris Preparation

A-1 Purpose

The purpose of this appendix is to identify the steps necessary to prepare fibrous and particulate debris for use in CIB test. Specifically, this section provides how to process the fiberglass insulation into a size distribution that is representative of the debris distribution projected to bypass the sump strainers in the case of a LOCA.

A-4 References

Ref.A-1 NRC Staff Review Guidance Regarding Generic Letter 2004-02 Closure in the Area of Strainer Head Loss and Vortexing, Mar 2008

Appendix-B Chemical Debris Preparation

B-1 Purpose

The purpose of this procedure is to manufacture safety related chemical debris for application to subsequent core inlet blockage testing performed on Mitsubishi Heavy Industries, Ltd. test module.

This procedural outline is general, but the production amount of chemical debris is specialized for core inlet blockage testing of the US-APWR.